



HAL
open science

Stabilization of polynuclear plutonium(IV) species by humic acid

Remi Marsac, Nidhu Lal Banik, Christian M. Marquardt, Jens Volker Kratz

► **To cite this version:**

Remi Marsac, Nidhu Lal Banik, Christian M. Marquardt, Jens Volker Kratz. Stabilization of polynuclear plutonium(IV) species by humic acid. *Geochimica et Cosmochimica Acta*, 2014, 131, pp.290 - 300. 10.1016/j.gca.2014.01.039 . hal-01904152

HAL Id: hal-01904152

<https://hal.science/hal-01904152>

Submitted on 24 Oct 2018

HAL is a multi-disciplinary open access archive for the deposit and dissemination of scientific research documents, whether they are published or not. The documents may come from teaching and research institutions in France or abroad, or from public or private research centers.

L'archive ouverte pluridisciplinaire **HAL**, est destinée au dépôt et à la diffusion de documents scientifiques de niveau recherche, publiés ou non, émanant des établissements d'enseignement et de recherche français ou étrangers, des laboratoires publics ou privés.

42 **Abstract**

43 Although the formation of tetravalent plutonium (Pu(IV)) polymers with natural organic
44 matter was previously observed by spectroscopy, there is no quantitative evidence of such
45 reaction in batch experiments. In the present study, Pu(IV) interaction with humic acid (HA)
46 was investigated at pH 1.8, 2.5 and 3, as a function of HA concentration and for Pu total
47 concentration equal to 6×10^{-8} M. The finally measured Pu(IV) concentrations ($[\text{Pu(IV)}]_{\text{aq}}$) are
48 below Pu(IV) solubility limit. Pu(IV)-HA interaction can be explained by the complexation of
49 Pu(IV) monomers by HA up to $[\text{Pu(IV)}]_{\text{aq}} \sim 10^{-8}$ M. However, the slope of the log-log
50 Pu(IV)-HA binding isotherm changes from ~ 0.7 to ~ 3.5 for higher $[\text{Pu(IV)}]_{\text{aq}}$ than $\sim 10^{-8}$ M
51 and at any pH. This result suggests the stabilization of hydrolyzed polymeric Pu(IV) species
52 by HA, with a 4:1 Pu:HA stoichiometry. This confirms, for the first time, previous
53 observations made by spectroscopy in concentrated systems. The humic-ion binding model,
54 Model VII, was introduced into the geochemical speciation program PHREEQC and was used
55 to simulate Pu(IV) monomers binding to HA. The simulations are consistent with other
56 tetravalent actinides-HA binding data from literature. The stabilization of a Pu tetramer
57 ($\text{Pu}_4(\text{OH})_8^{8+}$) by HA was proposed to illustrate the present experimental results for $[\text{Pu(IV)}]_{\text{aq}}$
58 $> 10^{-8}$ M. Predictive simulations of Pu(IV) apparent solubility due to HA show that the chosen
59 Pu(IV)-polymer has no impact for $\text{pH} > 4$. However, the comparison between these predictions
60 and recent spectroscopic results suggest that more hydrolyzed polymeric Pu(IV) species can
61 be stabilized by HA at $\text{pH} > 4$. Polymeric Pu(IV)-HA species might significantly enhance
62 Pu(IV) apparent solubility due to humics, which support a colloid-facilitated transport of this
63 low solubility element.

64

65 **Keywords**

66 Plutonium(IV), humic acid, complexation, polynuclear species, PHREEQC, Model VII.

67

1. INTRODUCTION

68

69 Humic colloids such as humic (HA) and fulvic (FA) acids are ubiquitous in natural
70 waters and present a high binding capacity for dissolved metal ions. It has been evidenced that,
71 in many cases, the mobility of metals in the environment was associated with colloidal
72 transport (Kretzschmar et al., 2005). This is particularly the case for plutonium (Pu), a highly
73 toxic and radioactive element. Significant amounts of Pu have been introduced into the
74 environment by nuclear weapons tests, for instance. The aqueous chemistry of plutonium is
75 rich and complex owing to its multitude of oxidation states ranging from +3 to +6 under
76 environmental conditions. Among those, Pu(IV) exhibits the largest stability field and is
77 considered as the most relevant oxidation state (Choppin, 2003). Although Pu(IV) was
78 considered as rather immobile due to its extremely low solubility (approximately 10^{-11} - 10^{-10}
79 M at pH=7; Neck and Kim, 2001), it shows a colloid-facilitated transport in presence of
80 humic colloids. This behavior was shown in migration experiments of humic-rich ground
81 water spiked with plutonium and other tetravalent metal ions like Th, Hf, and Zr (Artinger et
82 al., 2003a, 2003b). Because of the strong interaction with humic colloids, the concentration of
83 tetravalent trace metal ions in natural ground waters is directly related to the content of
84 dissolved organic matter (DOC) (Artinger et al., 2003a). Because humic and fulvic acids are
85 ubiquitous, they can play a significant role in the transport of plutonium to the biosphere
86 wherever plutonium has been released: from final and intermediate repositories, by hazardous
87 incident of nuclear power plants or facilities of the nuclear fuel cycle, or deposits from the
88 atmosphere by atmospheric bomb tests and reentry of artificial satellites containing atomic
89 batteries.

90 However, there are only a few experimental data about Pu(IV)-HA complexation that
91 can be used for geochemical and transport modeling to assess the hazard of plutonium for the
92 biosphere. Thanks to the very similar chemical properties of the f-elements, it is possible, for

93 a given redox state, to compare the stability constant with a ligand of different actinides (e.g.
94 Th, U, Np, Pu). Reiller et al. (2008) reviewed all the available tetravalent actinide (An(IV))
95 complexation data with HA and found a high consistency between them. More recent Pu(IV)-
96 HA binding studies are in relatively good agreement with the latter observation (Szabó et al.,
97 2010; Sasaki et al., 2012). In these references, Pu(IV)-HA interaction is described in terms of
98 complexation of mononuclear Pu with humic acid. However, a recent X-ray absorption
99 spectroscopic (XAFS) study has yielded evidence for the formation of polynuclear Pu(IV)
100 species with HA (Dardenne et al., 2009). This study suggested the formation of small
101 polynuclear species (i.e. a few Pu atoms) rather than large-sized Pu(IV)-(hydr)oxide particles
102 embedded in the organic matrix. Therefore, from the mechanistic point of view, it might be
103 possible to consider these entities as polynuclear complexes with humic acid rather than
104 precipitated nanophases stabilized in solution by organic polyelectrolytes.

105 An(IV) aquo ions have a high tendency to hydrolyse and to form amorphous
106 hydroxide solids e.g. ($\text{PuO}_{2(\text{am,hyd})}$). In the presence of these amorphous solid Pu(IV)-
107 (hydr)oxide, Pu(IV) can form eigen colloids (>1-2 nm) that can increase by two orders of
108 magnitude the apparent solubility of plutonium (Neck et al., 2007). Furthermore, in acidic
109 conditions, in the absence of solid (i.e. for solutions prepared below the saturation index of
110 $\text{PuO}_{2(\text{am,hyd})}$) it has been shown that Th(IV) and Pu(IV) aqueous speciation is controlled by
111 small polynuclear species (i.e. smaller than 1nm) (Walther et al., 2008, 2009). Contrary to
112 Th(IV), where well-defined species could be identified (i.e. from dimers to hexamers), Pu
113 simultaneously forms species of great variety. Therefore, on the one hand, intrinsic chemical
114 properties of Pu(IV) might explain why polynuclear species are formed with HA. On the other
115 hand, Pu(IV) eigen colloids might be stabilized by HA complexing groups. Indeed, it has been
116 shown in the case of Np(IV) that small organic acids can stabilize polynuclear species (Takao
117 et al., 2012), as well as in case of Pu(IV) with glycine (Knöpe and Soderholm, 2013). Earlier

118 studies have also observed the formation of polynuclear cation-HA species. In case of Al(III),
119 Browne and Driscoll (1993) and Sutheimer and Cabaniss (1997) considered the formation of
120 Al dimers to explain their complexation data. In case of Fe(III), there are spectroscopic
121 evidences for the formation of Fe di- or trimers with HA (Gustafsson et al., 2007; Karlsson
122 and Persson, 2010), although there are few complexation studies evidencing the formation of
123 polynuclear cation-HA in batch experiment. It is interesting to note that trivalent Al and Fe
124 present a high tendency to hydrolyze and to form polynuclear species in undersaturated
125 solutions with respect to solid phases (e.g. Hellman et al., 2006; Sarpola et al., 2013), as it is
126 the case for An(IV).

127 Although the stabilization of polynuclear Pu(IV)-HA species was suggested by
128 spectroscopy and is mechanistically plausible, there is so far no quantification of such
129 reactions in batch experiments. Indeed, previous studies aimed at investigating the interaction
130 of mononuclear An(IV) with HA, and the formation of humic colloids consisting of small
131 polynuclear metal species and HA was not considered. In contrast to all above mentioned
132 studies, the present work aims at verifying the formation of polynuclear-Pu(IV)-HA species.
133 The experiments were performed under acidic conditions in order to be able to study their
134 interaction in a large range of final Pu(IV) aqueous concentrations by minimizing the
135 formation of particulate Pu(IV)-(hydr)oxides or eigen colloids. A semi-mechanistical humic-
136 ion binding model (Model VII: Tipping et al., 2011) was introduced into the geochemical
137 speciation program PHREEQC (Parkhurst and Appelo, 1999) and was used as a tool to
138 discuss the relevance of polynuclear-Pu(IV)-HA species and their potential impact on Pu(IV)
139 apparent solubility due to HA complexation under acidic to neutral pH conditions.

140

141

142
143
144
145
146
147
148
149
150
151
152
153
154
155
156
157
158
159
160
161
162
163
164
165
166

2. MATERIALS AND METHODS

All chemicals were of pro analytical quality or better and were obtained from Merck (Darmstadt, Germany) or Riedel de Haen (Seelze, Germany). Milli-Q deionized water was used to prepare the solutions. The pH was measured by a pH meter (φ-310, Beckman, Germany) with a combined electrode (Beckman, Germany). The pH-meter was calibrated daily with certified commercial buffers at pH = 1, pH= 2, pH = 4, pH = 6 (Merck, Darmstadt, Germany).

2.1. Plutonium solution

For all the complexation studies, a 99.1 wt% ²³⁹Pu stock solution (6.0x10⁻⁴ M) , with small amounts of other isotopes (0.888 wt% ²⁴⁰Pu, 0.014 wt% ²⁴¹Pu) and known specific activities was used. The plutonium solution was prepared by diluting an aliquot of the stock solution with 1 M HClO₄. The solution then consisted of different oxidation states of plutonium. The tetravalent oxidation state of Pu was obtained by potentiostatic electrolysis in 1 M HClO₄. For the electrolysis, a homemade glass electrolytic cell with three separated compartments (U-shape) was used. The middle one was used as a working electrode (Pt), the right one contained a Pt counter electrode and the left one contained the reference electrode (Ag/AgCl). These compartments were connected with a potentiostat for obtaining a constant potential at the working electrode. A mixture of Pu oxidation sates was firstly electrolyzed at -0.6 Volt to obtain Pu(III), then Pu(IV) was fastly obtained from Pu(III) at 0.9 Volt. The purity of the Pu(IV) oxidation state was controlled by UV-Vis spectrometry (Cohen 1961). About 98 % of Pu(IV) and 2 % of Pu(IV) colloids were in the stock Pu solutions. The radioactivity concentration of ²³⁹Pu was measured by liquid scintillation counting (LSC) using the scintillation cocktail Ultima Gold XR (Packard) and LSC Tricab (Hewlett Packard).

167 **2.2. Humic acid (HA)**

168 The commercially available Aldrich humic acid (AHA) (sodium salt, charge 37 no.
169 01816-054) was purified and isolated as described in (Kim and Buckau, 1988; Kim et al.,
170 1990). The proton exchange capacity (PEC) is equal to 4.60×10^{-3} eq g⁻¹ (Kim and Buckau,
171 1988; Kim et al., 1990; Seibert et al., 2001). Although AHA is sometimes criticized as a
172 weak model for humic substances, its ion-binding behavior is rather similar to those of other
173 humic substances (Avena et al., 1999; Milne et al., 2001, 2003; Saito et al., 2005; Pourret et
174 al., 2007).

175

176 **2.3. Complexation experiments**

177 For the complexation experiments, HA and Pu(IV) were brought into contact at
178 different pH values (1.8-3.0). The pH of the samples was adjusted by using a minimum of 0.1
179 M HClO₄ or 0.1 M NaOH solutions. The Pu(IV) concentration was 6.6×10^{-8} M, and the humic
180 acid content was varied between 0.01 and 25 mg/L and all mixtures were shaken continuously
181 on an orbital shaker at 25°C. All experiments were performed at I = 0.1 M NaClO₄ under
182 aerobic condition at room temperature. Total sample volume was 10 mL in 20 mL vials. The
183 samples were filtrated using ultrafiltration (1 kDa pore size) after 24 hours, 3 days, 1 week,
184 and 2 weeks during preliminary complexation experiments. This preliminary study indicated
185 that complexation equilibrium was established after 1 week, so 1 week for sampling was
186 chosen in subsequent complexation experiments. The free Pu ion concentration was
187 determined by liquid scintillation counting (LSC) of the filtrates. In absence of humic acid,
188 the sorption of Pu(IV) on the filter material as well as on the vessel was determined and
189 considered in the evaluations. In the case of humic acid, less than 5 % of HA passed through
190 the 1kDa ultrafilter as measured by UV-Vis, which is being neglected in the present study.
191 Pourret et al. (2007) also investigated AHA complexation properties using 5kDa ultrafilter

192 and also detected negligible amount of organic matter passing through the membrane by total
193 organic carbon analysis. All experimental conditions and their results are given in the
194 supporting information (Table S1).

195

196 **2.4. Complexation modeling using PHREEQC and Model VII**

197 The Humic Ion-Binding Model VII (Tipping et al., 2011) is an improved version of
198 Model VI (Tipping, 1998). Both are based on the same equations but the total number of
199 different cation binding sites required to describe HA heterogeneity is decreased in Model VII
200 (= 50 versus 80 for Model VI). Model VI and VII are initially coupled with the inorganic
201 speciation code WHAM. It is here coupled with PHREEQC (version 2) developed by
202 Parkhurst and Appelo (1999), using the same strategy as used by Marsac et al. (2011) for
203 Model VI. PHREEQC is a computer code based on an ion-association aqueous model, which
204 was designed to perform speciation and saturation-index calculations in water.
205 Thermodynamic constants are taken from NEA thermodynamic database (Guillaumont et al.,
206 2003). Davies equation was used for activity coefficients calculation, being valid up to an
207 ionic strength of 0.1 M.

208 A thorough description of Model VII can be found in Tipping et al. (1998; 2011). The
209 model is a discrete binding site model which takes electrostatic interactions into account.
210 Only the aqueous cation (e.g. Pu^{4+}) and its first hydrolysis products (e.g. PuOH^{3+}) are
211 considered to bind to HA with the same binding constants. Eight sites are considered and
212 divided into an equal number of type A sites (commonly associated with carboxylic functional
213 groups) and type B sites (commonly associated with phenolic functional groups). There are n_A
214 (mol g^{-1}) type A sites and $n_A/2$ type B sites. An average value for n_A ($3.3 \times 10^{-3} \text{ eq g}^{-1}$) was
215 found by Tipping (1998) for various HA, leading to a PEC of $5.25 \times 10^{-3} \text{ eq g}^{-1}$, which is
216 relatively similar to the Aldrich HA used here and was not modified. Proton binding is

217 described by the two median intrinsic protonation constants (pK_A or pK_B ; negative decadic
218 logarithm of protonation constants K_A or K_B) and two parameters defining the spread of the
219 protonation constants around the median (ΔpK_A or ΔpK_B). The intrinsic equilibrium constants
220 for cation binding are defined by two median constants ($\log K_{MA}$ and $\log K_{MB}$), together with
221 parameters (ΔLK_{1A} and ΔLK_{1B}) that define the spread of the values around the medians.
222 However, satisfactory results are obtained by fixing $\Delta LK_{1A} = \Delta LK_{1B} = 0$. The work of
223 Carbonaro and Di Toro (2007) showed that the relative binding strength of a metal cation with
224 monodentate ligands is the same as those for protons. This concept was applied to carboxylic
225 and phenolic HA groups in Model VII by Tipping et al. (2011). It is assumed that

$$226 \quad \log K_{MB} = \log K_{MA} \cdot (pK_B/pK_A) \quad (1)$$

227 which reduces the number of adjustable parameters necessary to describe metal complexation
228 by HA. A fraction of the type A and type B monodentate sites can form bi- (f_{bi}) and tridentate
229 (f_{tri}) sites. The stability constants of these bi- and tridentate sites are defined by the sum of the
230 $\log K$ values of the monodentate sites of which they are constituted. A small part of the
231 stability constants of multidentate groups are increased by the ΔLK_2 parameter, the so-called
232 "strong binding site term" (Tipping, 1998). In Model VII, ΔLK_2 is commonly attributed to the
233 participation of additional HA ligands in the complex, such as the nitrogen-containing groups.
234 However, Marsac et al. (2011) suggested that, in case of hard Lewis acids (e.g. trivalent
235 lanthanides), a high ΔLK_2 value might be attributed to a chelation effect. ΔLK_2 is also the
236 parameter of the HA site heterogeneity. An elevation of ΔLK_2 increases the range of the
237 stability constants covered by the HA sites, thus increasing the heterogeneity of HA regarding
238 cations binding.

239 An electrical double layer, where only counter-ions can accumulate, is defined. The
240 double layer thickness is set by the Debye-Hückel parameter $\kappa = (3.29 \times 10^9 \times I^{1/2})^{-1}$ (Appelo
241 and Postma, 2005), where I is the ionic strength (mol L^{-1}). The distribution of ions between

242 the diffuse layer and the bulk solution is calculated by a Donnan model. The electrostatic
243 correction is represented by an empirical equation which mimics the Boltzmann factor:

$$244 \quad \text{Exp}(-zF\psi/RT) = \exp(-2PzZ \log_{10}I) \quad (2)$$

245 where P is an adjustable parameter, z is the ion charge, Z is the net humic acid charge (eq g⁻¹),
246 I is the ionic strength (mol L⁻¹), ψ is the surface potential (V), T is the temperature (K), F is
247 the Faraday constant and R is the gas constant. In PHREEQC, the surface area (SA) is
248 required:

$$249 \quad SA = ZF \times (0.1174 \times I^{1/2} \times \sinh(F\psi/2RT))^{-1} \quad (3)$$

250 By combining eq.2 and eq.3, a relationship between SA and P is obtained. For I = 0.1
251 M, P = -196, whatever Z is valued, $|PZ \log_{10}I|$ becomes low and the sinh can be approximated
252 by a linear function (Taylor's approximation). Indeed, R² = 0.996 is found when the sinh term
253 versus Z is fitted with a linear function. The following equation is obtained:

$$254 \quad SA = F \times (0.1174 \times I^{1/2} \times P \log_{10}I)^{-1} \quad (4)$$

255 which depends only on the ionic strength. We found SA~20000 m² g⁻¹ for I = 0.1 M.
256 Although rather unrealistic, such high surface area is the consequence of translating the
257 empirical electrostatic correction equation used in the initial version of Model VII into the
258 double layer theory. Such high SA were also used in different studies, where Model V
259 (Tipping and Hurley 1992) and VI were introduced into PHREEQC (Appelo and Postma,
260 2005; Liu et al., 2008; Marsac et al., 2011). To our knowledge there is no better solution at
261 present. Note that the present approximation is only valid for any Z when both $|\log_{10} I|$ and $|P|$
262 are low. For lower I than 0.1 M or more negative P values (e.g. -330 as in Model VI), the
263 linearization of the sinh function is only valid for a narrower range of Z values. It means that
264 SA depends also on the pH. In this case, Marsac et al. (2011) simply chose a value of SA in
265 PHREEQC/Model VI that fitted best the simulated HA proton titration simulated with

266 WHAM/Model VI, between pH 2 and 10. A summary of all Model VII parameters are given
267 in the supporting information (Table S2).

268 As can be deduced from the latter description of Model VII, the description of HA
269 binding properties is comparable with solid surface complexation modeling. Humic acid
270 conformation changes with the physico-chemical conditions are not explicitly described.
271 However, their impact on cation complexation might be included implicitly in the different
272 binding parameters used. The physical state of the humic, i.e. probably coagulated for pH < 2
273 in the present study or even voluntarily insolubilized (Weber et al., 2006), is not supposed to
274 impact the determination of cation-HA binding parameters for Model VII. It will be further
275 illustrated in the present study.

276

277 **2.5. Parameter estimation with PhreePlot**

278 PhreePlot (Kinniburgh and Cooper, 2009) contains an embedded version of
279 PHREEQC and is mainly used to produce certain types of high quality geochemical plots
280 using PHREEQC such as pH-Eh diagrams, for instance. However, PhreePlot also includes a
281 parameter optimization procedure, which fits automatically the model to the experimental
282 data by minimizing the weighted sum of squares of the residuals. A modified Marquardt-
283 Levenberg procedure (Powel, 1965) was applied, which provides incertitude on the estimated
284 parameters. In the present study, PhreePlot was requested to fit $\log [\text{Pu}]_{\text{aq}}$ by optimizing \log
285 $K_{\text{MA}}(\text{Pu(IV)})$, $\Delta\text{LK}_2(\text{Pu(IV)})$ as well as the formation constant of polynuclear Pu(IV) species
286 with HA. Numeric tags can substitute numbers in the PHREEQC section of the PhreePlot
287 input file. In Model VII, every Pu(IV)-HA complexation constants being calculated from \log
288 $K_{\text{MA}}(\text{Pu(IV)})$ and $\Delta\text{LK}_2(\text{Pu(IV)})$, a readable form of Model VII must be written for PhreePlot
289 using the keyword “numericTags” to make possible the automatic determination of
290 optimizing $\log K_{\text{MA}}(\text{Pu(IV)})$ and $\Delta\text{LK}_2(\text{Pu(IV)})$ parameters.

3. RESULTS AND DISCUSSION

3.1. Plutonium(IV) interaction with humic acid

Fig. 1 shows the solubility of Pu(IV) as a function of pH calculated with PHREEQC from the following equation (Guillaumont et al., 2003):



The Pu(IV) concentrations at equilibrium ($[\text{Pu(IV)}]_{\text{aq}}$) in the present Pu-HA complexation experiments are below the solubility curve. Dotted lines represent the uncertainty on Pu(IV) solubility, as determined from the uncertainties of hydrolysis constants and solubility product. Therefore, no precipitation or Pu(IV)-colloids is expected. This statement might be, however, debatable at pH = 3 because here, $[\text{Pu(IV)}]_{\text{aq}}$ are higher than the minimum uncertainty limit of the Pu(IV) solubility.

Pu(IV)-HA complexation data were first treated as follows:



$$K_{\text{exp}} = \frac{[\text{Pu}_n\text{HA}]}{[\text{Pu}]_{\text{eq}}^n [\text{HA}]} = \frac{[\text{PuHA}] / n}{[\text{Pu}]_{\text{eq}}^n [\text{HA}]} \quad (7)$$

where K_{exp} is a conditional constant, $[\text{Pu}]_{\text{eq}}$ (in mol L⁻¹) and $[\text{PuHA}]$ (mol g⁻¹ of HA) denotes the experimentally determined concentrations of Pu in the filtrate and in the retentate, respectively, and n is the stoichiometry of the reaction normalized to one HA site. $[\text{HA}]$ is defined here as the PEC (eq g⁻¹) of HA, i.e. the total site concentration, because it is not possible to determine precisely the free HA site concentration due to both HA site heterogeneity and the lack of knowledge about Pu(IV)-HA interaction. This implies that n and K_{exp} are only estimates of the stoichiometry and conditional formation constants of reaction 6. Applying some rearrangements to eq. 7, one obtains a Freundlich-type isotherm equation:

$$\log \frac{[\text{PuHA}]}{[\text{HA}]} = \log K_{\text{exp}} + \log n + n \log [\text{Pu}]_{\text{eq}} \quad (8)$$

315 Fig. 2 presents the amount of Pu(IV) complexed to HA (in mol eq⁻¹) as a function of
316 Pu(IV) equilibrium concentration ([Pu(IV)]_{eq}), i.e. the Pu(IV)-HA binding isotherm. The
317 concentration of plutonium humic complexes (Pu(IV)-HA) increases with pH due to the
318 decrease of proton competition for HA binding groups in the complexation reaction. From
319 low (10⁻⁹ M) to intermediate Pu concentrations (10⁻⁸ M, [Pu(IV)]_{eq}), the slope of the log-log
320 isotherm is with a value of 0.73 significantly below 1 (illustrated for pH 3 in Fig. 2). This is
321 explained with the heterogeneity of HA sites for Pu(IV) complexation. The latter pH and
322 metal loading effects have been widely described for many cations complexation by humic
323 substances, and a slope below 1 is commonly observed for cations binding to humic even at
324 low site occupancy (e.g. Benedetti et al., 1995). However, for [Pu(IV)]_{aq} > 10⁻⁸ M, the mean
325 slope of the isotherm of all pH values drastically increases to a value of 3.5 (3.8 as illustrated
326 at pH = 3; Fig. 2). At pH = 3, this observation might be firstly attributed to the precipitation of
327 Pu(IV)-(hydr)oxides or at least to formation of Pu(IV) eigencolloids because experimental
328 [Pu(IV)]_{aq} values are near to the Pu(IV) solubility limit. However, the same high slope (3.94)
329 is observed at a more acidic pH value of 1.8, where it is clear that Pu(IV) does not precipitate
330 in the range of [Pu(IV)]_{aq} studied here. It is well established that Pu(IV) is the most stable Pu
331 redox state in the presence of HA even under anaerobic conditions (Marquardt et al., 2004;
332 Dardenne et al., 2009). Furthermore, the present experiments were performed in contact with
333 air preventing the formation of Pu(III). Therefore, the slope of the isotherm being larger than
334 1 is not a result of oxidation state transformation during the experiment, but might be
335 attributed to the presence of Pu(IV) polynuclear species. Because Pu(IV) solubility was
336 determined by ultrafiltration at 3 kDa (pore size: 1-2 nm; Neck and Kim, 2001) to separate
337 Pu(IV)-HA complexes from the solution, the increase of the amount of Pu(IV) in the HA
338 fraction of our experiments can only be attributed to polynuclear Pu(IV) species associated to
339 the HA colloids. Indeed, earlier studies showed no significant difference between 3 kDa and 1

340 kDa ultrafilter for the separation of Pu(IV)-HA complexes. If we consider a linear binding
341 behavior of polynuclear Pu(IV) species to HA, the slope of the isotherm equal to 3.5 suggests
342 the formation of 3:1 or 4:1 Pu-HA complexes, presuming a polynuclear Pu(IV) species binds
343 to one HA site. When considering the 4:1 stoichiometry, at pH=3, a condition constant of log
344 $K_{\text{exp}}=27.3$ can be estimated for the humate complexation reaction (6). However, due to HA
345 heterogeneity, binding of polynuclear Pu(IV) species to HA might not be linear, and would
346 imply a higher degree of Pu(IV) polynucleation. This stoichiometry is actually more likely an
347 average value because a large variety of polynuclear species might be formed at the same time
348 with HA, as it has been observed by Walther et al. (2009), in solution under similar conditions,
349 but below the solubility limit.

350

351 **3.2. Modeling with PHREEQC/model VII**

352 The preceding interpretations are tested with the humic-ion binding model, Model VII.
353 Phreeplot was used to calibrate Pu-HA binding parameters in Model VII fitting the present
354 experimental data. This automatic fitting procedure also provides the uncertainty of the
355 determined parameters. The optimized model parameters are presented in Table 1 and are
356 compared with the estimated values determined by Stockdale et al. (2011) that were used here
357 as initial values for the fit. Log K_{MA} (i.e. the main binding parameter) and ΔLK_2 (i.e. the
358 strong sites binding parameter) were found equal to 3.9 ± 0.2 and 1.7 ± 0.5 , respectively. These
359 results are not significantly different from the estimated values of Stockdale et al. (2011) and
360 validate the estimation method. For Th(IV), Tipping et al. (2011) have determined log
361 $K_{\text{MA}}(\text{Th(IV)}) = 3.58$ and $\Delta\text{LK}_2(\text{Th(IV)}) = 0.23$, which are slightly lower than the presently
362 determined values for Pu(IV). But when applying the uncertainties from the Pu(IV) fit on the
363 Th(IV) values, both data set can be regarded as very similar within the range of uncertainties.
364 The simulated results are also illustrated as binding isotherms in Fig. 3 (dotted lines), when

365 considering only the binding of Pu(IV)-monomers to HA. The model can reproduce relatively
 366 well the results for $[Pu(IV)]_{aq}$ below approximately 10^{-8} M. Obviously, the model cannot
 367 reproduce the change in the slope of the binding isotherm at $[Pu(IV)]_{aq}$ higher than 10^{-8} M, for
 368 the reasons explained before.

369 The reaction of polynuclear An(IV) species stabilization by carboxylic ligands was
 370 written as follows by Takao et al. (2012):



$$372 \quad K_{poly} = \frac{[(RCOO)_a An_b O_c H_d][H^+]^{(c+d)}}{[RCOO^-]^a [An^{4+}]^b} \quad (10)$$

373 where a, b, c, and d are, respectively, equal to 12, 6, 8 and 4 in case of formate (R = H, log
 374 $K_{poly} = 42.7$ at I = 0.62 M) and acetate (R = CH₃, log $K_{poly} = 52.0$ at I = 0.66M), for An = Np.
 375 In case of Pu(IV)-HA complexation, the stoichiometry seems to be approximately 4:1,
 376 according to the present experiments. The pH dependence of the reaction is, however, very
 377 difficult to evaluate because of HA site heterogeneity, the competition between Pu(IV) and H⁺
 378 for these sites and the hydrolysis of Pu(IV) formed with HA. Furthermore, Walther et al.
 379 (2009) observed a large variety of the number of Pu atoms in the polynuclear species. As
 380 mentioned before, the stabilization of polynuclear Pu(IV) species by HA should probably be
 381 described by a distribution of polynuclear Pu(IV) species. Unfortunately, it appears not
 382 possible for the moment to provide a more precise description of the formation of polynuclear
 383 Pu-HA species by modeling, because the distribution of the polynuclear species is unknown.
 384 The modeling exercise in the present paper is based on several assumptions. Although it can
 385 be regarded as a rough estimation of this complex system, it will help us as an illustration to
 386 discuss the relevance of such polynuclear species under environmental conditions. Because
 387 $Pu(OH)_2^{2+}$ is the dominant species in solution (see Fig. S1) from which polynuclear
 388 compounds are formed via edge sharing, the formation reaction of tetra-Pu(IV)-HA
 389 complexes was introduced in Model VII as follows:



391 Only the mono-carboxylic sites defined in Model VII were considered, which
392 represent 43.5% of the total HA carboxylic groups because the fraction of bi- and tridentate
393 sites is fixed. Indeed, the 4:1 stoichiometry of the complexes would not have been respected
394 when considering the complexation of Pu-tetramer to bi- and tridentate HA sites as defined in
395 Model VII. The logarithm of the formation constant of reaction (11) was found to be 31.4 ± 0.4 .
396 This value is higher than the conditional formation constant estimated by the slope analysis
397 (e.g. 27.3 at pH = 3; Fig. 2) because, (i) the latter one did not take into account the HA sites
398 occupancy by Pu and protons, and (ii) only 43.5% of HA sites are involved according to
399 Model VII definition of monodentate sites. Although this tetramer complex presents a high
400 positive charge, it might be compensated by the overall HA negative charge. The
401 complexation of relatively highly charged polynuclear species to humics are generally
402 required to model data obtained in acidic condition: $\text{Al}_2(\text{OH})_4^{4+}$ (Sutheimer and Cabaniss,
403 1997), Fe_2O^{4+} (Gustafsson et al., 2007) or $\text{Fe}_3\text{O}_2^{5+}$ (Marsac et al., 2013). Note that in the
404 present model, the Pu-tetramer-HA formation reaction suggests HA sites as templates for
405 bridge bonding between hydroxy-Pu(IV) ions, which is consistent with the previous trivalent
406 cation-humics studies. The results of the fit are presented in Fig. 3. The model can reproduce
407 the data at pH 1.8 relatively well whereas more deviations are observed at pH 3. By
408 increasing the pH, the distribution of hydrolyzed polymeric An(IV) species increases
409 (Walther et al., 2009). The deviation observed at pH = 3 might be a direct consequence of the
410 strong simplification of the system in the model by introducing only one type of polynuclear
411 Pu(IV) species. Nevertheless, considering such (over)simplification, this approach can
412 reproduce the experimental results relatively well.

413

414

415 3.3. Comparison with An(IV)-HA binding data from literature

416 Reiller et al. (2008) compiled and re-interpreted the An(IV)-HA (An = Th, U, Pu)
417 complexation data available in the literature. They recalculated conditional complexation
418 constants as follows:



$$420 {}^{\text{HA}}\beta(\text{An}^{4+}) = \frac{[\text{AnHA}]}{[\text{An}^{4+}]_{\text{aq}}[\text{HA}]} \quad (13)$$

421 where [HA] is calculated from the proton exchange capacity (eq g⁻¹). The concentration of the
422 An⁴⁺ aquo cation [An⁴⁺]_{aq} are very low and are calculated from the total aqueous An(IV)
423 concentration ([An(IV)]_{aq}) measured experimentally and the hydrolysis constants (β_{1,n}) of the
424 considered An(IV):

$$425 [\text{An}^{4+}]_{\text{aq}} = [\text{An(IV)}]_{\text{aq}} \times \left(1 + \sum_{n=1}^4 \frac{\beta_{1,n}}{[\text{H}^+]^n} \right) = [\text{An(IV)}]_{\text{aq}} \alpha_{\text{An}} \quad (14)$$

426 The site reaction coefficient α_{An} considers all hydrolysis reactions of the An⁴⁺ cation. They
427 found a high consistency between all tetravalent actinides by only using the hydrolysis
428 constants of U(IV) for all An(IV) hydrolysis reactions and they derived the following
429 equation:

$$430 \log {}^{\text{HA}}\beta(\text{An}^{4+}) = (3.26 \pm 0.10)\text{pH} + (0.14 \pm 0.67). \quad (15)$$

431 The present experimental results were recalculated with the approach of Reiller et al.
432 for [Pu(IV)]_{aq} < 10⁻⁸ M (i.e. where Pu(IV) binds to HA as monomeric species) and are plotted
433 in Fig. 4 as well as the results of eq. (15) (Reiller et al., 2008) for different pH. The
434 consistency between the present log ^{HA}β(Pu⁴⁺) data for [Pu(IV)]_{aq} < 10⁻⁸ M and eq. 15 shows
435 that our results are in excellent agreement with literature. In at least part of our experiments
436 (i.e. for pH < 2), HA has coagulated. This result suggests that the physical state of the humic
437 has no significant impact on its binding properties, which was already observed in earlier
438 studies for An(III) or Fe(III) (Kim et al., 1993; Weber et al., 2006). Note that because of the

439 low solubility of An(IV), experiments performed at high pH had low $[\text{An(IV)}]_{\text{tot}}$. Therefore,
440 the slope of eq. (15) takes also into account, implicitly, the effect of low metal loading of HA.

441 Simulations with PHREEQC/Model VII were performed as a function of the pH using
442 10 mg/L of HA and $[\text{Pu(IV)}]_{\text{tot}}$ 10 times below the solubility limit. Such conditions are
443 commonly investigated to avoid $\text{An(OH)}_{4(\text{am})}$ precipitation or colloid formation in the sample.
444 The contribution of Pu(IV) tetramer is also negligible. The results of the simulations were
445 recalculated according to eq. (13) – (14) and taking into account the default PEC value of HA
446 in Model VII. These results are illustrated together with the results according to eq. (15)
447 (Reiller et al., 2008) in Fig. 4. Although Pu(IV)-HA binding parameters in Model VII were
448 calibrated only with our experimental results obtained under acidic conditions (i.e. $\text{pH} \leq 3$), the
449 evolution of $\log {}^{\text{HA}}\beta(\text{Pu}^{4+})$ with pH is well described up to $\text{pH}=7$, attributing to Model VII
450 some efficiency as a predictive tool. The uncertainty of Model VII parameters presently
451 determined (bold dotted lines) are comparable with the uncertainty of $\log {}^{\text{HA}}\beta(\text{An}^{4+})$
452 determined by Reiller et al. (2008). As mentioned earlier, only the binding of Pu^{4+} and
453 PuOH^{3+} to HA were considered. This finding is opposed to the Charge Neutralization Model
454 (CNM), commonly used to describe actinides complexation by humic acids (Kim and
455 Czerwinski, 1996). This model requires the binding of several hydrolysis products of Pu(IV)
456 to HA to simulate the pH dependence of $\log {}^{\text{HA}}\beta(\text{Pu}^{4+})$. However, the CNM does not take into
457 account the heterogeneity of HA and cannot reproduce the effect of the metal loading, for
458 instance. Model VII considers the presence of strong chelating sites in low amount. Due to the
459 low solubility of $\text{PuO}_{2(\text{am,hyd})}$, $[\text{Pu(IV)}]_{\text{aq}}$ becomes very low under near neutral conditions.
460 Therefore, in such conditions, Pu(IV) is considered to be complexed by chelating sites of HA.
461 It has been shown that chelating ligands can inhibit An(IV) hydrolysis (e.g. Jeanson et al.,
462 2010) even under alkaline conditions. The description of Pu(IV)-HA interaction provided by
463 Model VII might be considered as relatively consistent from the mechanistic point of view.

464 Model VII underestimates $\log^{HA}\beta(\text{Pu}^{4+})$ for $\text{pH}>7$, suggesting that more hydrolyzed Pu(IV)
465 species, such as $\text{Pu}(\text{OH})_2^{2+}$, might have to be considered as species bound to HA. However,
466 preliminary tests (not presented here) showed that $\text{Pu}(\text{OH})_2^{2+}$ Model VII parameters had to be
467 optimized independently from PuOH^{3+} , which lead to an increase in the number of adjustable
468 parameters. Furthermore, a binding isotherm up to high loading cannot be obtained
469 experimentally for $\text{pH}>7$ because of the low solubility of $\text{PuO}_{2(\text{am,hyd})}$. Therefore, it is not
470 possible to constrain $\text{Log } K_{\text{MA}}$ and ΔLK_2 for $\text{Pu}(\text{OH})_2^{2+}$ independently. Predictive modeling
471 of Pu(IV) solubility in the presence of HA would give very different results depending on the
472 choice of the couple $\text{Log } K_{\text{MA}}/\Delta\text{LK}_2$. Furthermore, it does not seem very clear if additional
473 parameters (i.e. the complexation of more hydrolyzed Pu(IV) monomers) have to be
474 considered in the calculations. Indeed, cation complexation constants with HA multidentate
475 sites in Model VII are subjected to a large uncertainty. For instance, the uncertainty associated
476 with the formation of a bidentate complex is twice the sum of the corresponding monodentate
477 ones. The strong sites are additionally subjected to the incertitude associated to ΔLK_2 . This
478 can somewhat be seen, for instance on figure 4: at low pH, the simulation was performed at
479 higher $[\text{Pu}(\text{IV})]_{\text{tot}}$ than at high pH. Therefore, at low pH, the incertitude on $\log^{HA}\beta(\text{Pu}^{4+})$ is
480 almost not visible on figure 4 because Pu(IV) speciation with HA is dominated by lower
481 denticity sites than at higher pH, where the strong HA multidentate sites are dominant. A
482 slight modification of already existing parameters describing the strong sites in Model VII
483 might improve significantly the simulation for An(IV) complexation to HA without
484 considering additional parameters. However, the present study does not aim at revising Model
485 VII. Therefore, the present discussion will be limited to $\text{pH}<7$, where only the complexation
486 of Pu^{4+} and PuOH^{3+} binding to HA can reproduce relatively well the experimental results.
487
488

489 3.4. Relevance of poly-Pu(IV)-HA species under circumneutral conditions

490 Dardenne et al. (2009) have studied the Pu(IV)-HA formation by XAFS in a humic-
491 rich groundwater ($\sim 70 \text{ mgC L}^{-1}$) at $\text{pH} \sim 7$ and a Pu concentration of $1.4 \times 10^{-4} \text{ M}$. In presence of
492 HA, this Pu(IV) concentration is approximately 10^6 times higher than Pu(IV) solubility limit
493 in 0.1 M NaCl aqueous solution at $\text{pH} = 7$. In the experiment, a precipitation of potential
494 Pu(IV)-(hydr)oxide was not observed and the good quality of the data confirms that a
495 significant fraction of the Pu(IV) remained in solution. Indeed, to be able to record an
496 Extended X-ray Absorption Fine Structure (EXAFS) spectrum up to $k = 11 \text{ \AA}^{-1}$, Pu(IV)
497 concentrations of $\sim 100 \text{ ppm}$ are typically required in the solution, which corresponds to $\sim 10^{-4}$
498 M of Pu(IV). The EXAFS showed a significant Pu-Pu signal. Furthermore, the Pu L3-edge
499 XANES (X-ray Absorption Near Edge Structure) was very similar to aqueous Pu(IV) (i.e. in a
500 solution at $\text{pH} = 0$) and differed strongly from solid $\text{PuO}_{2(\text{am,hyd})}$ or from colloidal Pu(IV) in
501 solution (Walther et al., 2009). From the mechanistic point of view, it might be possible to
502 consider these entities as polynuclear complexes with humic rather than precipitated
503 nanophases. In neutral to alkaline pH conditions, when the solution is in contact with solid
504 $\text{PuO}_{2(\text{am,hyd})}$, the formation of Pu(IV) eigencolloids can only increase Pu(IV) apparent
505 solubility up to $10^{-8.3 \pm 0.5} \text{ M}$ (Neck et al., 2007). These results evidenced that natural organic
506 matter can inhibit the precipitation of $\text{PuO}_{2(\text{am,hyd})}$ by the formation of small polynuclear
507 Pu(IV) humate species. Although there is no available systematic solubility study of Pu(IV) in
508 the presence of HA, the large amount of Pu remaining in solution in the experiments of
509 Dardenne et al. (2009) suggests also that HA can enhance Pu apparent solubility. This might
510 also impact Pu mobility in organic-rich environments, provided that a significant amount of
511 Pu-HA does not aggregate.

512 The Pu(IV) apparent solubility in presence of HA was simulated with
513 PHREEQC/Model VII for $2 < \text{pH} < 7$, i.e. in a range of pH conditions where Model VII gave

514 satisfactory results, in a 0.1 M NaCl solution containing 140 mg L⁻¹ of HA. This [HA]
515 corresponds to 70 mg L⁻¹ of dissolved organic carbon (DOC), considering that carbon
516 represents 50 wt.% of HA. These conditions reproduce roughly the Gorleben groundwater
517 (Marquardt et al., 2004) and they were investigated here as an illustration rather than in sense
518 of a prediction. Aqueous Pu(IV) and Pu(IV)-HA species were considered as dissolved species.
519 Results are presented in Fig. 5. When considering only the formation of monomeric Pu(IV)-
520 HA species, HA can significantly enhance Pu(IV) apparent solubility for pH>2.5. At pH=7,
521 the apparent solubility in presence of HA is underestimated by more than 3 orders of
522 magnitude, compared with the sample studied by XAFS by Dardenne et al. (2009). Note also
523 that the precipitation of metallic (hydr)oxides in the presence of HA might lead to highly
524 amorphous or nanometric (hydr)oxides with an enhanced solubility. This was the case, for
525 instance, for Fe(III) whose (hydr)oxides formed in the presence of HA had a higher solubility
526 than ferrihydrite, an amorphous Fe(III)-hydroxide (Weber et al., 2006; Marsac et al., 2013).
527 However, the increase of Fe(III) solubility in presence of HA did not exceed one order of
528 magnitude. When considering additionally the formation of polynuclear Pu(IV)-HA species,
529 Pu(IV) apparent solubility increases in presence of HA by 1.5 log units at pH=3. The
530 arbitrarily chosen Pu(IV) tetramer to illustrate the present experimental results between pH 1
531 and 3 has no impact for pH > 4 and cannot explain the XAFS results of Dardenne et al. (2009).
532 Actually, the fact that the Pu(IV) tetramer has only an impact in conditions quite similar to the
533 present experiments is rather comforting because its occurrence at pH > 5 would have been
534 highly questionable. Nevertheless, these simulations show that the stabilization of a more
535 hydrolyzed Pu_n(OH)_m species than Pu₄(OH)₈⁸⁺ by HA should be considered in the model to
536 produce simulations consistent with spectroscopy.

537 To our best knowledge, the only experimental An(IV) solubility data in the presence
538 of organic matter were performed with U(IV) in the presence of carbonates (Cachoir et al.,

539 2003; Delécaut et al., 2004). Such data are relevant for performance assessment of nuclear
540 waste disposal but it is difficult to determine precisely which chemical mechanisms hide
541 behind the observed behavior. Under these conditions, U(IV) can easily be oxidized to U(VI)
542 and carbonates can compete with organic matter. Indeed, Reiller et al. (2008) analyzed the
543 data by geochemical speciation modeling and discussed the factors that could have an
544 influence on uranium concentration in the HA-containing solution. The finally presented
545 simulated results, although very promising, still underestimated U solubility data. However,
546 the stabilization of polynuclear U(IV)-HA species could not be tested because there was no
547 clear evidence of such species in the literature. By comparison with the present results for
548 Pu(IV), the formation of polynuclear actinide(IV)-HA might be an alternative explanation for
549 the deviation observed between experimental and modeling results. However, it is very
550 difficult to estimate precisely the thermodynamic parameters of such reaction yet, especially
551 under near neutral pH conditions.

552

553

4. CONCLUSION

554 The present study on Pu(IV) humate complexation at $\text{pH} < 3$ yields evidence for the
555 complexation of both mono- and polynuclear Pu(IV) species to HA, at conditions where no
556 Pu(IV) precipitation is expected. Model VII is used to simulate Pu(IV) monomers binding to
557 HA. The simulations are consistent with other tetravalent actinides-HA binding data from
558 literature (Reiller et al., 2008). The stabilization of a Pu tetramer ($\text{Pu}_4(\text{OH})_8^{8+}$) by HA is
559 proposed to illustrate Pu(IV)-HA interaction in conditions where polynuclear Pu(IV)-HA
560 species are formed. Although a robust model considering both the formation of mono- and
561 polynuclear Pu(IV) complexes with HA cannot be derived from the present and previous
562 studies, such polynuclear species are expected to have an impact under relevant conditions in
563 the environment. They significantly increase the Pu(IV) apparent solubility due to HA

564 complexation, more than by humate complexation of monomeric Pu(IV) species. Due to their
565 similar chemical properties, comparable mechanisms are also expected for other tetravalent
566 actinides, such as U(VI) and Np(IV). Such a mechanism of humate or fulvate complexation
567 strongly supports a transport of An(IV) as a humic colloid-borne species as observed in
568 migration experiments (Artinger et al., 2003a,b). Therefore, further studies should be
569 dedicated to the colloidal stability of An(IV)-HA (i.e. mono- and polynuclear) complexes.
570 More generally, the stabilization of polynuclear cations by HA seems to be a relevant
571 mechanisms at least for cations presenting a high tendency for hydrolysis such as An(IV),
572 Al(III) (Browne and Driscoll, 1993; Sutheimer and Cabaniss, 1997) or Fe(III) (Gustafsson et
573 al., 2007; Karlsson and Persson, 2010). This might impact on the fate of these elements in the
574 environment but might also affect other elements through the competition for organic matter
575 binding sites.

576

577 **Acknowledgements.**

578 We would like to thank the ‘German Ministry of Economy and Technology’ (Projekt 02 E
579 9309 5 and 02 E 1579653’) for financial support. We thank the three anonymous reviewers
580 and the associate editor, Dr. Marc Norman, for their helpful comments.

581

582 **References**

583 Appelo C. and Postma D. (2005) *Geochemistry, groundwater and pollution*. second ed. Taylor
584 & Francis, New York, p. 595.

585 Artinger R., Buckau G., Zeh P., Gereadts K., Vancluysen J., Maes A. and Kim J. I. (2003a)
586 Humic colloid mediated transport of tetravalent actinides and technetium. *Radiochim.*
587 *Acta* **91**, 743-750.

588 Artinger R., Kuczewski B., Marquardt C. M., Schäfer T., Seibert A. and Fanghänel T. (2003b)
589 Humic colloid mediated transport of plutonium studied by column experiments.

590 Internal report, institut for nuclear waste disposal, Forschungszentrum Karlsruhe,
591 Karlsruhe, Germany.

592 Avena M. J., Vermeer A. W. P. and Koopal L. K. (1999) Volume and structure of humic acids
593 studied by viscometry pH and electrolyte concentration effects. *Colloids and Surfaces A*
594 **151**, 213-224.

595 Benedetti M. F., Milne C. J., Kinniburgh D. G., van Riemsdijk W. H. and Koopal L. K.
596 (1995) Metal-ion binding to humic substances: application of the non-ideal competitive
597 adsorption model. *Environ. Sci. Technol.* **29**, 446-457.

598 Browne B. A. and Driscoll C. T. (1993) pH dependent binding of aluminum by a fulvic acid.
599 *Environ. Sci. Technol.* **27**, 915-922.

600 Cachoir C., Lemmens K., Van den Berghe S. and Van Iseghem P. (2003) UO₂ dissolution in
601 Boom Clay conditions. *J. Nucl. Mater.* **321**, 49-59.

602 Carbonaro R.F. and Di Toro D.M. (2007) Linear free energy relationships for metal–ligand
603 complexation: Monodentate binding to negatively-charged oxygen donor atoms.
604 *Geochim. Cosmochim. Acta* **71**, 3958–3968.

605 Choppin G. R. (2003) Actinide speciation in the environment. *Radiochim. Acta* **91**, 645-650.

606 Cohen D. (1961) The absorption spectra of plutonium ion in perchloric acid solutions. *J.*
607 *Inorg. Nucl. Chem.* **18**, 211-218.

608 Dardenne K., Seibert A. , Denecke M. A. and Marquardt C. M. (2009) Plutonium(III,IV,VI)
609 speciation in Gorleben groundwater using XAFS. *Radiochim. Acta* **97**, 91–97.

610 Delécaut G., Maes N., De Canniere P. and Wang L. (2004) Effect of reducing agents on the
611 uranium concentration above uranium(IV) amorphous precipitate in Boom Clay pore
612 water. *Radiochim. Acta* **92**, 545-550.

613 Guillaumont R., Fanghänel Th., Fuger J., Grenthe I., Neck V., Palmer D.A. and Rand M.H.
614 (2003) Update on the chemical thermodynamics of uranium, neptunium, plutonium,
615 americium and technetium. OECD/NEA Data Bank, Eds., *Chemical Thermodynamics*
616 vol. 5, Elsevier, Amsterdam.

617 Gustafsson J. P., Persson I., Kleja D. B. and van Schaik J. W. J. (2007) Binding of iron(III) to
618 organic soils: EXAFS spectroscopy and chemical equilibrium modeling. *Environ. Sci.*
619 *Technol.* **41**, 1232–1237.

620 Hellman H., Laitinen R. S., Kaila L., Jalonen J. E., Hietapelto V. K., Jokela J., Sarpola A. T.
621 and Rämö J. H. (2006) Identification of hydrolysis products of $\text{FeCl}_3 \cdot 6\text{H}_2\text{O}$ by ESI-MS.
622 *J. Mass Spectrom.* **41**, 1421-1429.

623 Jeanson A., Ferrand M., Funke H., Hennig C., Moisy P., Solari P. L., Vidaud C. and Auwer
624 C.D. (2010) The role of transferrin in actinide(IV) uptake: comparison with iron(III).
625 *Chem. Eur. J.* **16**, 1378-1387.

626 Karlsson T. and Persson P. (2010) Coordination chemistry and hydrolysis of Fe(III) in a peat
627 humic acid studies by X-ray absorption spectroscopy. *Geochim. Cosmochim. Acta* **74**,
628 30-40.

629 Kim J. I., Rhee D. S., Wimmer H., Buckau G. and Klenze R. (1993) Complexation of
630 trivalent actinide ions ($\text{Am}^{3+}, \text{Cm}^{3+}$) with humic acid: A comparison of different
631 experimental methods. *Radiochim. Acta* **62**, 35-43.

632 Kim J. I. and Buckau G. (1988) Report RCM 02188, Institut für Radiochemie der TU 182
633 München. 183.

634 Kim J. I. and Czerwinski K. R. (1996) Complexation of metal ions with humic acid: metal ion
635 charge neutralization model. *Radiochim. Acta* **73**, 5-10.

636 Kim J. I., Buckau G., Li G. H., Duschner H. and Psarros N. (1990) Characterization of humic
637 acid and fulvic acids from Gorleben groundwater. *Fresenius J. Anal. Chem.* **338**, 245-
638 252.

639 Kinniburgh D. G. and Cooper D. M. (2009) PhreePlot: Creating graphical output with
640 PHREEQC. <<http://www.phreeplot.org>>.

641 Knope K. E. and Soderholm L. (2013) Plutonium(IV) cluster with a hexanuclear
642 $[\text{Pu}_6(\text{OH})_4\text{O}_4]^{12+}$ core. *Inorg. Chem.*, in press. DOI: 10.1021/ic4007185

643 Kretzschmar R. and Schäfer T. (2005) Metal retention and transport on colloidal particles in
644 the environment. *Element* **1**, 205-210.

645 Liu D. J., Bruggeman C. and Maes N. (2008) The influence of natural organic matter on the
646 speciation and solubility of Eu in Boom Clay porewater. *Radiochim. Acta* **96**, 711–720.

647 Marquardt C. M., Seibert A., Artinger R., Denecke M. A., Kuczewski B., Schild D. and
648 Fanghänel Th. (2004) The redox behaviour of plutonium in humic rich groundwater.
649 *Radiochim. Acta* **92**, 617-623.

650 Marsac R., Davranche M., Gruau G., Bouhnik-Le Coz M and Dia A. (2011) An improved
651 description of the interactions between rare earth elements and humic acids by
652 modelling. *Geochim. Cosmochim. Acta* **75**, 5625-5637.

653 Marsac R., Davranche M., Gruau G., Dia A., Pédrot M., Bouhnik-Le Coz M. and Briant N.
654 (2013) Iron competitive effect on REE binding to organic matter: implications with
655 regards to REE patterns in waters. *Chem. Geol.* **342**, 119-127.

656 Milne C. J., Kinniburgh D. G. and Tipping E. (2001) Generic NICA-Donnan Model
657 parameters for proton binding by humic substances. *Environ. Sci. Technol.* **35**, 2049-
658 2059.

659 Milne C. J., Kinniburgh D. G., Van Riemsdijk W. H. and Tipping E. (2003) Generic NICA-
660 Donnan Model parameters for metal-ion binding by humic substances. *Environ. Sci.*
661 *Technol.* **37**, 958-971.

662 Neck V. and Kim J. I. (2001) Solubility and hydrolysis of tetravalent actinides. *Radiochim.*
663 *Acta* **89**, 1-16.

664 Neck V., Altmaier M., Seibert A., Yun J.I., Marquardt C.M. and Fanghänel Th. (2007)
665 Solubility and redox reactions of Pu(IV) hydrous oxide: Evidence for the formation of
666 PuO_{2+x} (s, hyd). *Radiochim. Acta* **95**, 193–207.

667 Parkhurst D. L. and Appelo C. A. J. (1999) User's guide to PHREEQC (Version 2) - a
668 computer program for speciation, batch reaction, one-dimensional transport and inverse
669 geochemical calculation. Water-resources Investigation Report 99–4259, USGS, Denver,
670 Colorado, p. 312.

671 Pourret O., Davranche M., Gruau G. and Dia A. (2007) Rare earth complexation by humic
672 acid. *Chem. Geol.* **243**, 128-141.

673 Powell M. J. D. (1965) A method for minimizing a sum of squares of non-linear functions
674 without calculating derivatives. *The Computer Journal* **7**, 303–307. Also see VA05 in
675 the HSL Archive, ftp://ftp.numerical.rl.ac.uk/pub/hsl_catalogs/archive/catalog.pdf.

676 Reiller P., Evans N. D. M. and Szabó G. (2008) Complexation parameters for the
677 actinides(IV)-humic acid system: a search for consistency and application to laboratory
678 and field observations. *Radiochim. Acta* **96**, 345-358.

679 Saito T., Nagasaki S., Tanaka S. and Koopal L. K. (2005) Electrostatic interactions model for
680 ion binding to humic substances. *Colloids and Surfaces A* **265**, 104-113.

681 Sarpola A. T., Hietapelto V. K., Jalonen J. E., Jokela J. and Rämö J. H. (2013) Comparison of
682 hydrolysis products of $\text{AlCl}_3 \cdot 6\text{H}_2\text{O}$ in different concentrations by electrospray
683 ionization time of flight mass spectrometer (ESI TOF MS). *Intern. J. Environ. Anal.*
684 *Chem.* **86**(13), 1007-1018.

685 Sasaki T., Aoyama S., Yoshida H., Kulyako Y., Samsonov M., Kobayashi T., Takagi I.,
686 Miyasoedov B. and Moriyama H. (2012) Apparent formation constants of Pu(IV) and
687 Th(IV) with humic acids determined by solvent extraction method. *Radiochim. Acta*
688 **100**, 737–745.

689 Seibert A., Mansel A., Marquardt C. M., Keller H., Kratz J. V. and Trautmann N. (2001)
690 Complexation behaviour of neptunium with humic acid. *Radiochim. Acta* **89**, 505–510

691 Stockdale A., Bryana N. D. and Loft S. (2011) Estimation of Model VII humic binding
692 constants for Pd^{2+} , Sn^{2+} , U^{4+} , NpO_2^{2+} , Pu^{4+} and PuO_2^{2+} . *J. Environ. Monit.* **13**, 2946-
693 2950.

694 Sutheimer S. H. and Cabaniss S. E. (1997) Aluminum binding to humic substances
695 determined by high performance. *Geochim. Cosmochim Acta* **61**(1), 1-9.

696 Szabó G., Guzzi J., Reiller P., Miyajima T. and Bulman R. A. (2010) Effect of ionic strength
697 on complexation of Pu(IV) with humic acid. *Radiochim. Acta* **98**, 13–18.

698 Takao K., Takao S., Scheinost A. C., Bernhard G. and Hennig C. (2012) Formation of soluble
699 hexanuclear neptunium(IV) nanoclusters in aqueous solution: Growth termination of
700 actinide(IV) hydrous oxides by carboxylates. *Inorg. Chem.* **51**, 1336-1344.

701 Tipping E. (1998) Humic ion-binding model VI: an improved description of the interactions
702 of protons and metal ions with humic substances. *Aquat. Geochem.* **4**, 3-48.

703 Tipping E. and Hurley M. A. (1992) A unifying model of cation binding by humic substances.
704 *Geochim. Cosmochim. Acta* **56**, 3627–3641.

705 Tipping E., Lofts S. and Sonke J. (2011) Humic ion-binding Model VII: a revised
706 parameterisation of cation-binding by humic substances. *Environ. Chem.* **8**, 225-235.

707 Walther C., Fuss M. and Büchner S. (2008) Formation and hydrolysis of polynuclear Th(IV)
708 complexes – a nano-electrospray mass spectrometry study. *Radiochim. Acta* **96**, 411-
709 425.

710 Walther C., Rothe J., Brendebach B., Fuss M., Altmaier M., Marquardt C. M., Büchner S.,
711 Cho H.-R., Yun J.-I. and Seibert A. (2009) New insights in the formation processes of
712 Pu(IV) colloids. *Radiochim. Acta* **97**, 199-207.

713 Weber T., Allard T., Tipping E. and Benedetti M. (2006) Modelling iron binding to organic
714 matter. *Environ. Sci. Technol.* **40**, 7488-7493.

715

716 **Table and Figure caption**

717

718 **Table 1.** Pu(IV)-HA binding parameters in Model VII ($\log K_{MA}$ and ΔLK_2) presently
719 determined. Estimated values by Stockdale et al. (2011) and fitted parameters for Th(IV)-HA
720 complexation (Tipping et al., 2011) are also shown for comparison.

721 **Figure 1.** Comparison between Pu(IV) concentration determined experimentally at
722 equilibrium in the presence of HA at pH=1.8, 2.5 and 3 ($[Pu]_{tot} \sim 6 \cdot 10^{-8} M$, $0.025 < [HA] < 25$ mg
723 L^{-1}) and Pu(IV) solubility limit calculated from Pu(IV) hydrolysis and solubility product
724 given in Guillaumont et al. (2003) (plain line) with the corresponding uncertainty (dashed
725 lines), in 0.1M of $NaClO_4$.

726 **Figure 2.** Pu(IV) binding to HA as function of $\log [Pu(IV)]_{aq}$ at pH 1.8, 2.5 and 3. A "break"
727 in the binding isotherm is observed and is illustrated at pH 3 by fitting the data with two linear
728 functions, $[HA] = 0.025-25$ mg/L, $I = 0.1M NaClO_4$, contact time = 1 week, Ultrafiltration
729 (1kDa).

730 **Figure 3.** Comparison between experimental and modeling results of Pu(IV)-HA binding
731 considering or not the stabilization of Pu(IV) tetramer by HA.

732 **Figure 4.** Evolution An^{4+} -HA conditional stability constant versus pH as calculated from eq.
733 15 (Reiller et al. 2008; solid line within the uncertainty presented as dashed lines). The present
734 experimental data (grey squares) and simulated results with Model VII (bold line) are also
735 presented for comparison, associated with the uncertainty on Model VII parameters (bold
736 dotted lines).

737 **Figure 5.** Simulated Pu(IV) solubility versus pH in a 0.1M of NaCl solution containing
738 $140 mg L^{-1}$ of HA or no HA. The experimental condition studied by XAFS (Dardenne et al.,
739 2009), where polynuclear Pu(IV)-HA species were evidenced, is also shown for comparison.

740

741

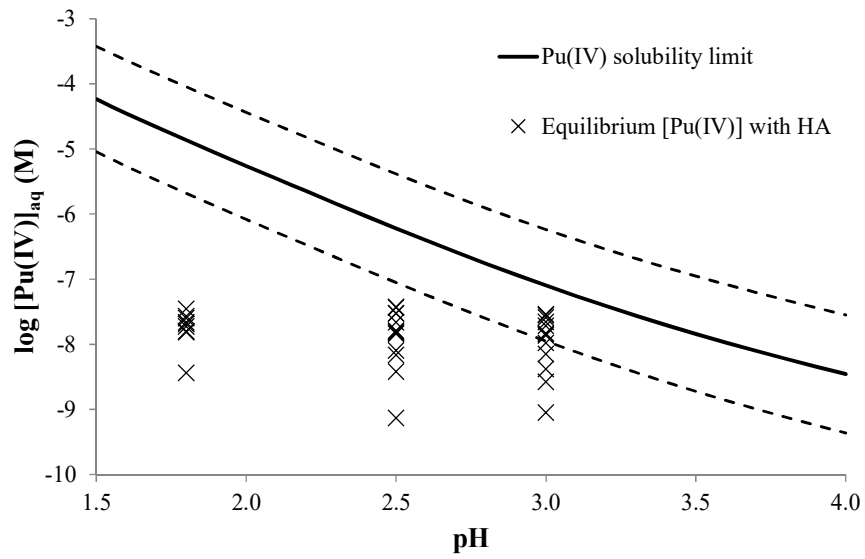
	Pu(IV) (present study)	Pu(IV) (estimated)	Th(IV)
Log K_{MA}	3.9±0.2	4.08	3.58
ΔLK_2	1.7±0.5	1.85	0.23

742

743

Table 1

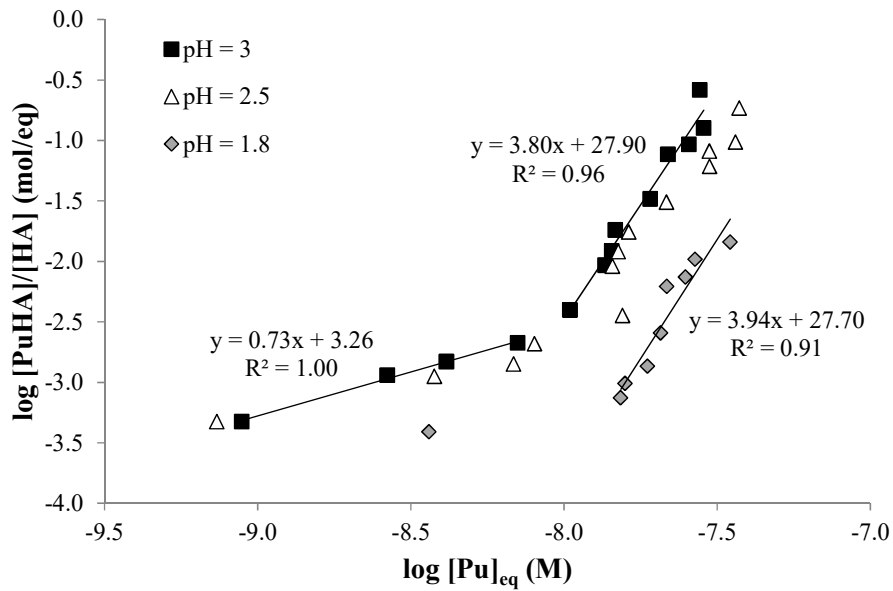
744



745

746

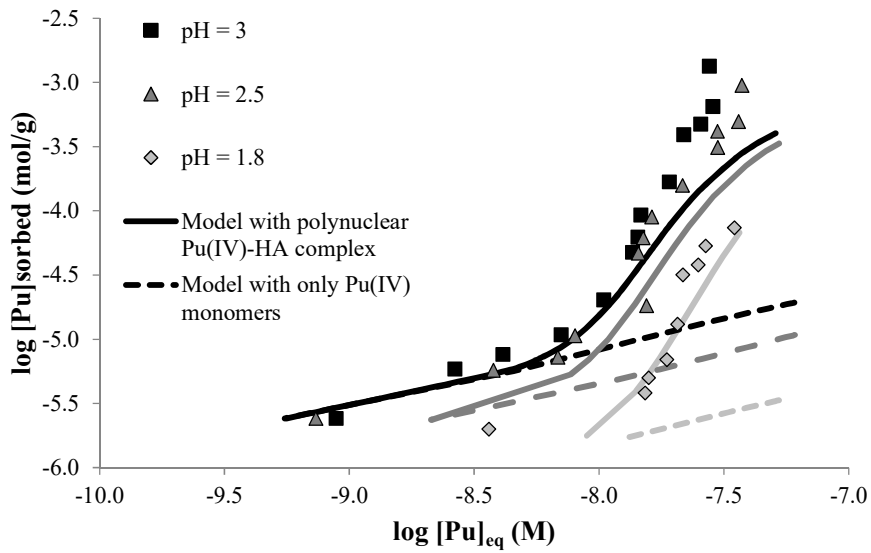
Figure 1



747

748

Figure 2

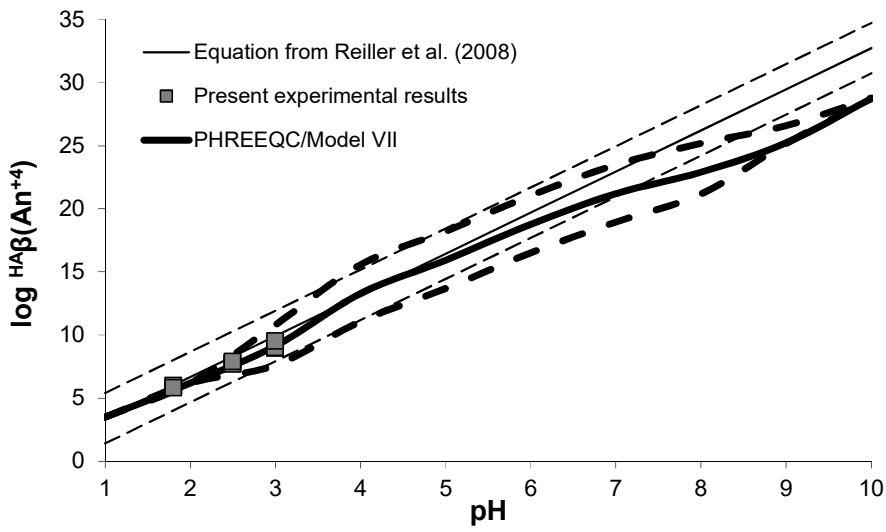


749

750

751

Figure 3



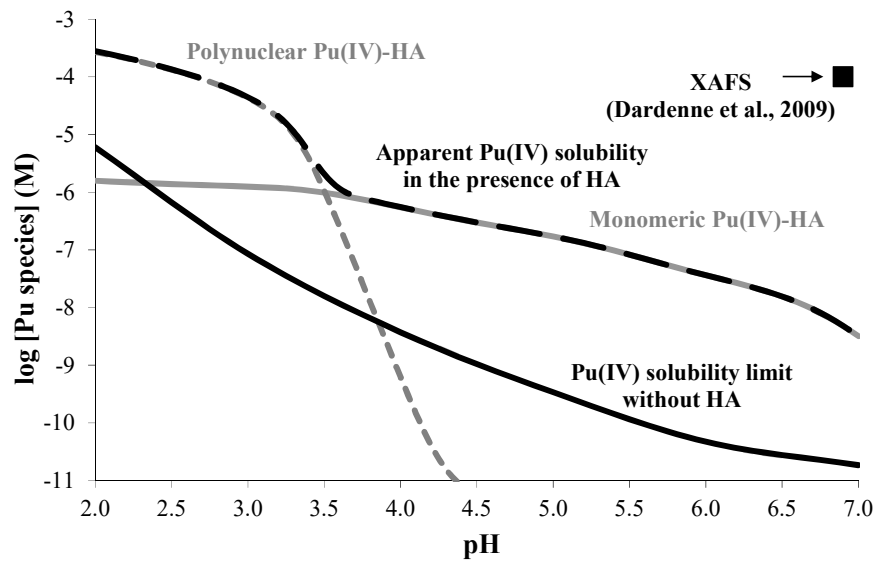
752

753

754

755

Figure 4



756

757

758

Figure 5